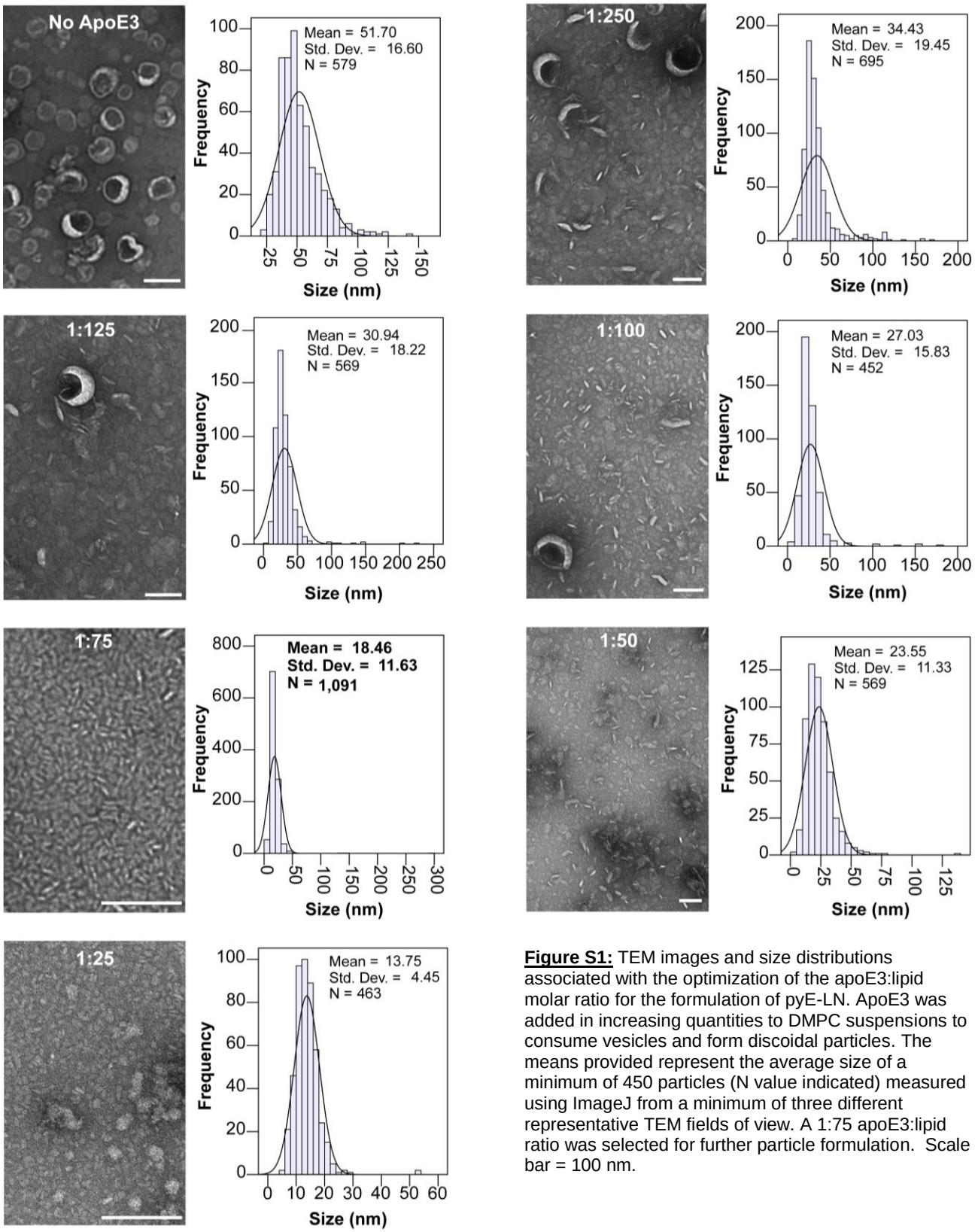

Figure S1: TEM images and size distributions associated with the optimization of the apoE3:lipid molar ratio for the formulation of pyE-LN. ApoE3 was added in increasing quantities to DMPC suspensions to consume vesicles and form discoidal particles. The means provided represent the average size of a minimum of 450 particles (N value indicated) measured using ImageJ from a minimum of three different representative TEM fields of view. A 1:75 apoE3:lipid ratio was selected for further particle formulation. Scale bar = 100 nm.

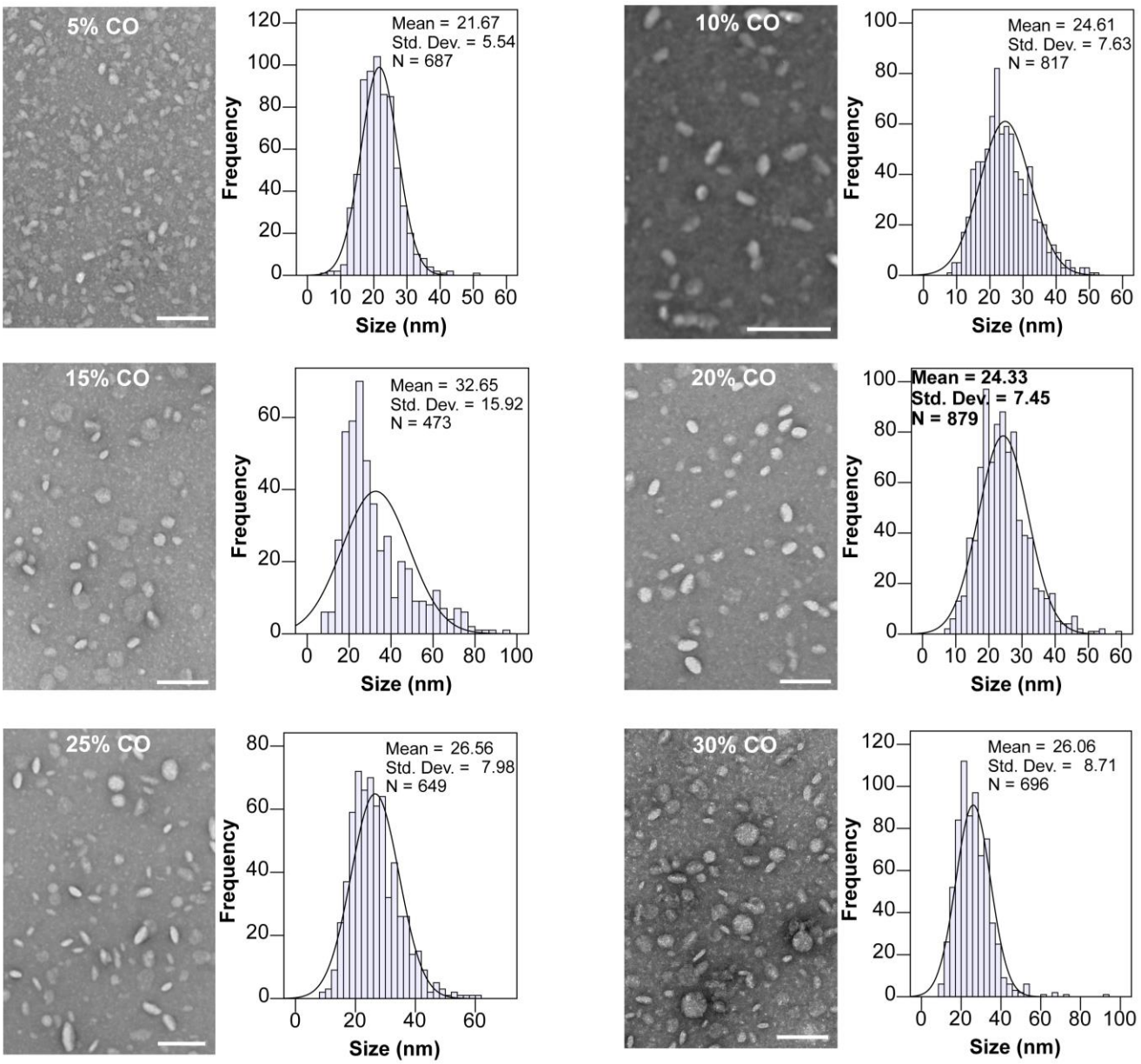

Figure S2: TEM images and size distributions associated with the optimization of the CO/lipid molar ratio, where percentages indicate CO quantity with respect to total moles of lipid. CO was titrated into DMPC lipid films prior to sonication and addition of apoE3 in a 1:75 apoE3:DMPC molar ratio. An increasing addition of CO resulted in a morphological change from discoidal to ellipsoidal and spherical particles, with high CO loading resulting in highly heterogenous particle morphology. The means provided represent the average size of a minimum of 450 particles (N value indicated) measured using ImageJ from a minimum of three different representative TEM fields of view. A loading of 20 molar% CO with respect to total lipid was selected to formulate pyE-LN-CO. Scale bar = 100 nm.

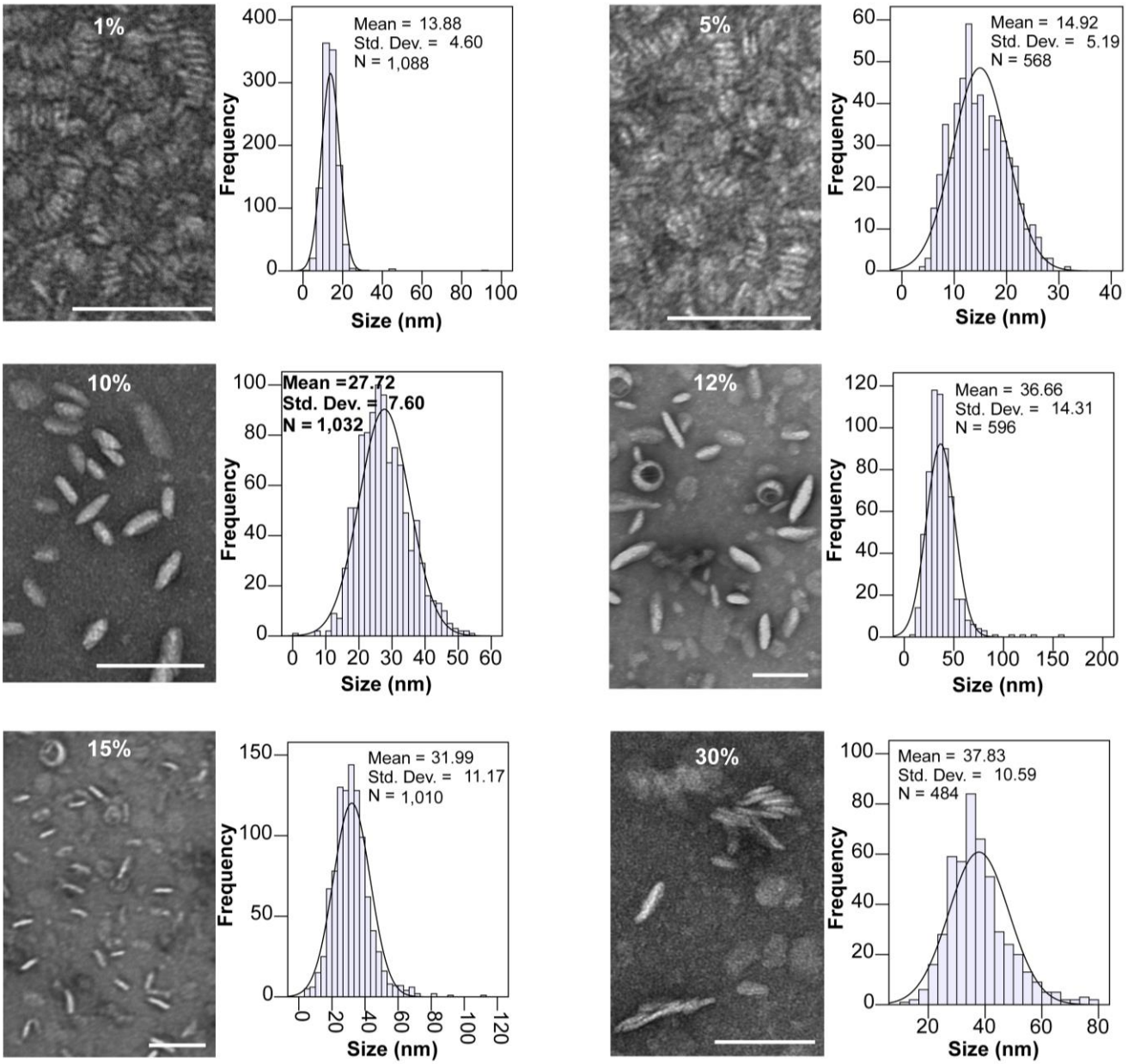

Figure S3: TEM images and size distributions associated with the titration of porphyrin-lipid into pyE-LN-D formulations. Percentages indicate the molar fractions of the total lipid content comprised of porphyrin-lipid. Increasing the porphyrin-lipid fraction increased the mean particle size, which represents the average size of 450 particles (N value indicated) measured using ImageJ from a minimum of three different representative TEM fields of view. A 10% porphyrin-lipid/90% DMPC lipid composition was selected to formulate optimized pyE-LN-D. Scale bar = 100 nm.

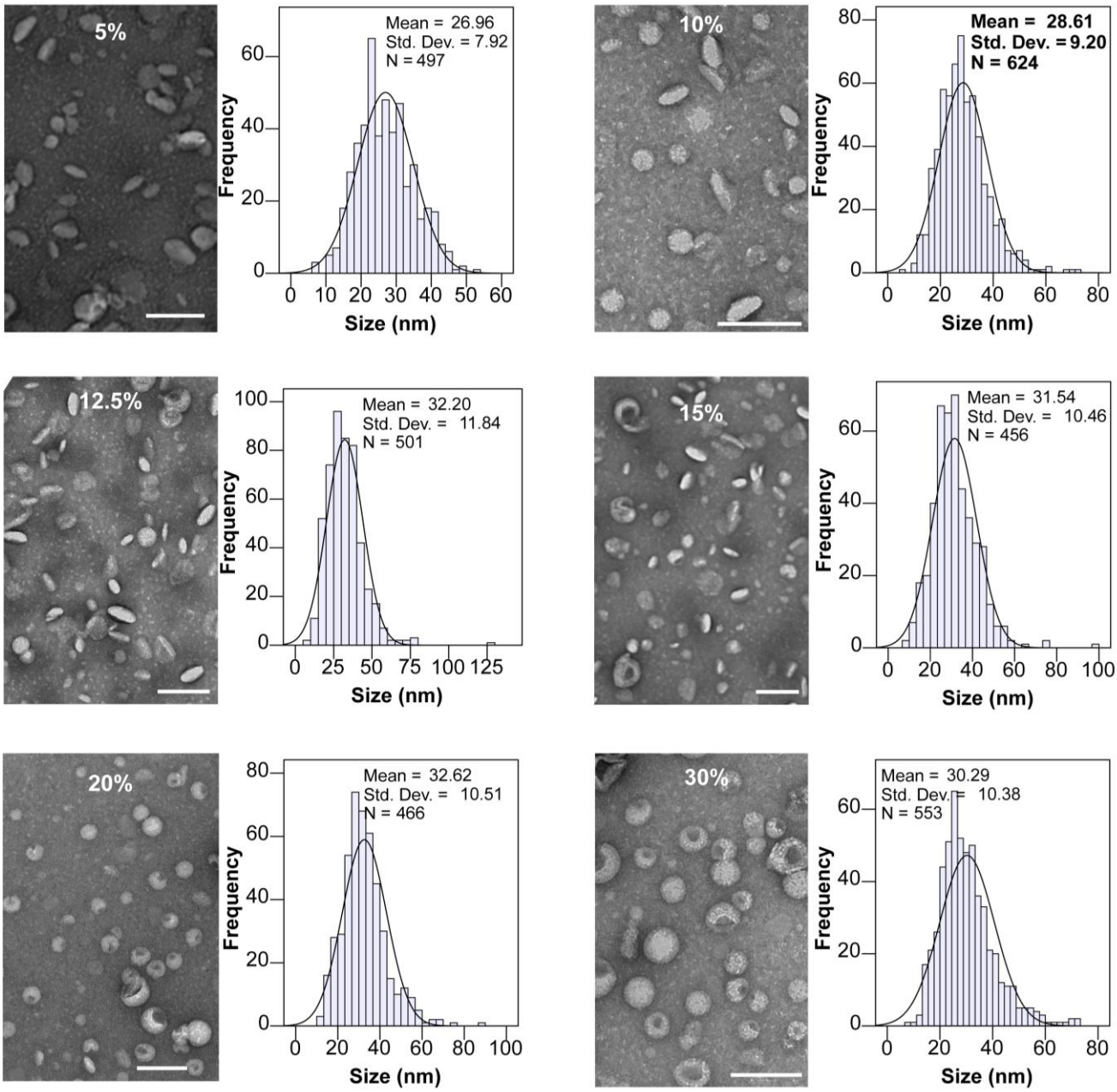

Figure S4: TEM images and size distributions associated with the titration of porphyrin-lipid into pyE-LN-CO formulations. Percentages indicate the molar fractions of the total lipid content comprising porphyrin-lipid. Increasing the porphyrin-lipid fraction increased the number of vesicles formed as observed by TEM. The means provided represent the average size of a minimum of 450 particles (N value indicated) measured using ImageJ from a minimum of three different representative TEM fields of view. A 10% porphyrin-lipid/90% DMPC lipid composition was selected to formulate optimized pyE-LN-D. Scale bar = 100 nm.

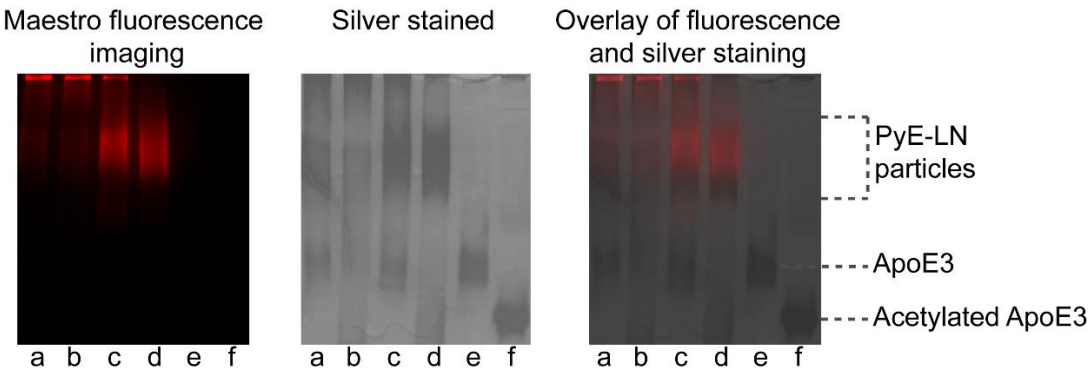

Figure S5: Native polyacrylamide gel electrophoresis of (a) pye-LN-CO, (b) pyE-LN-CO-Ac, (c) pyE-LN-D, (d) pyE-LN-D-Ac, (e) ApoE3, and (f) ApoE3-Ac. The gel was imaged on a CRi Maestro fluorescence imaging system to detect porphyrin signal (616-661 nm excitation, 675 nm longpass emission, 750 ms exposure), subsequent to which the gel was silver stained to visualize apoE3 bands (grey). Image co-registration demonstrates overlap in fluorescence and protein bands suggesting that the porphyrin-lipid and apoE3 in the particle suspensions are co-assembled.

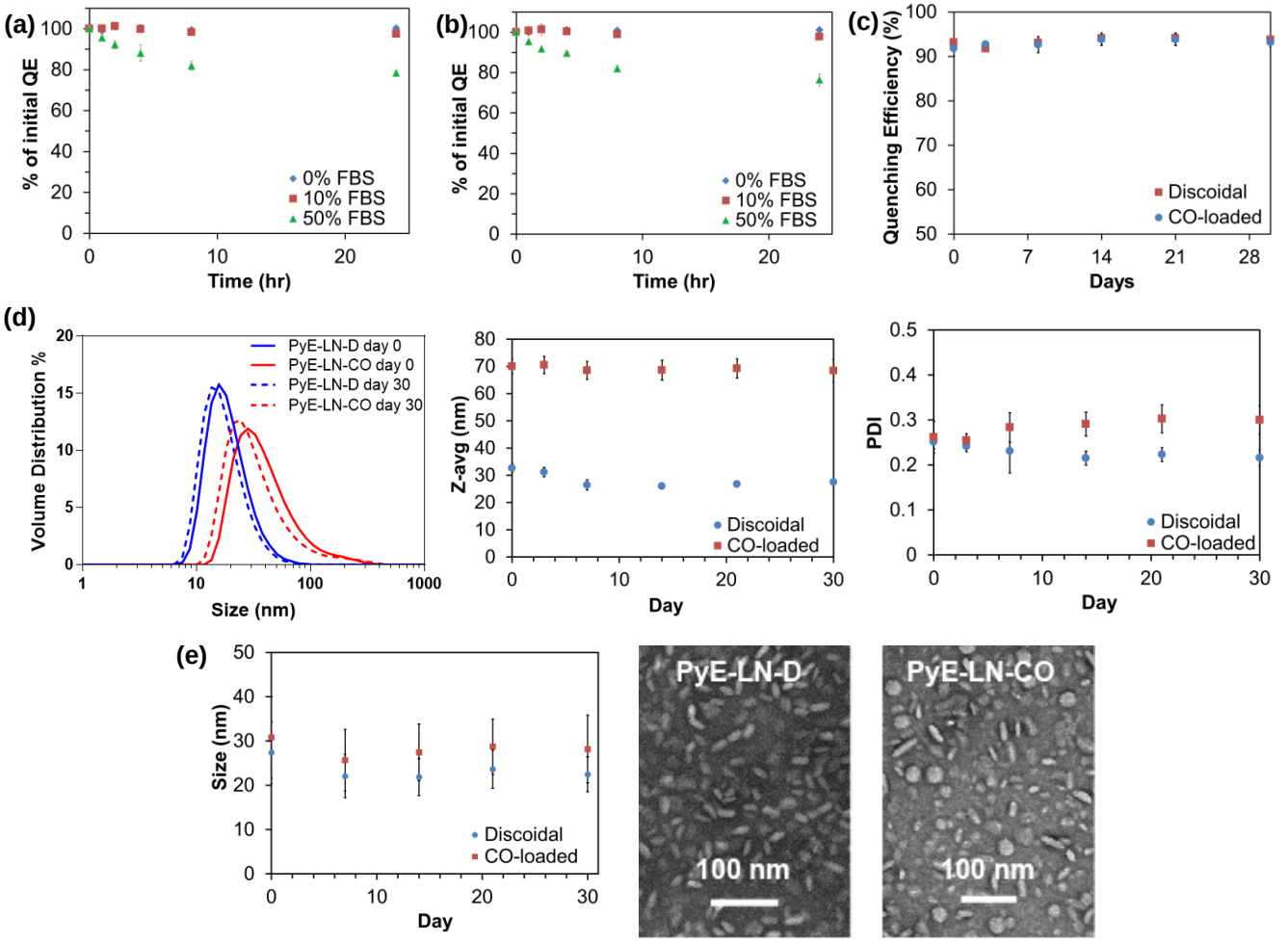

Figure S6: Serum and storage stability of pyE-LN nanoparticles. Serum stability of (a) pyE-LN-D and (b) pyE-LN-CO was evaluated by monitoring the fluorescence quenching efficiency (600-750 nm, 410 nm excitation) of particles dispersed in FBS solutions over a 24 hour period at 37ºC. Storage stability of aqueous particle solutions was assessed via quenching efficiency (c), DLS (d), and TEM (e) measurements, conducted on three samples stored at 4ºC for 30 days. No significant change (independent samples t-test, 3 samples) in quenching efficiency or increase in particle size (by TEM and DLS) were observed between Day 0 and Day 30. All data points represent the mean of three samples ± standard deviation. TEM size measurements are presented as the average of 450 measurements (150 from each of three samples, measured with ImageJ) ± standard deviation.

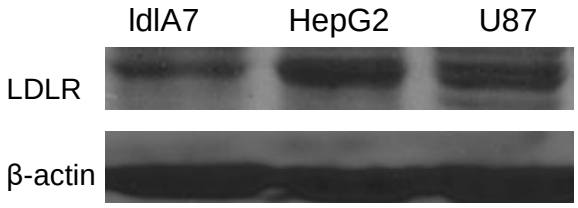

Figure S7: Western blot of ldlA7, U87 and HepG2 cell lysates using anti-LDLR and β-actin antibodies. U87s were found to have high expression of LDLR, similar to that of HepG2 (positive control for LDLR expression), while ldlA7 demonstrated lower LDLR expression.

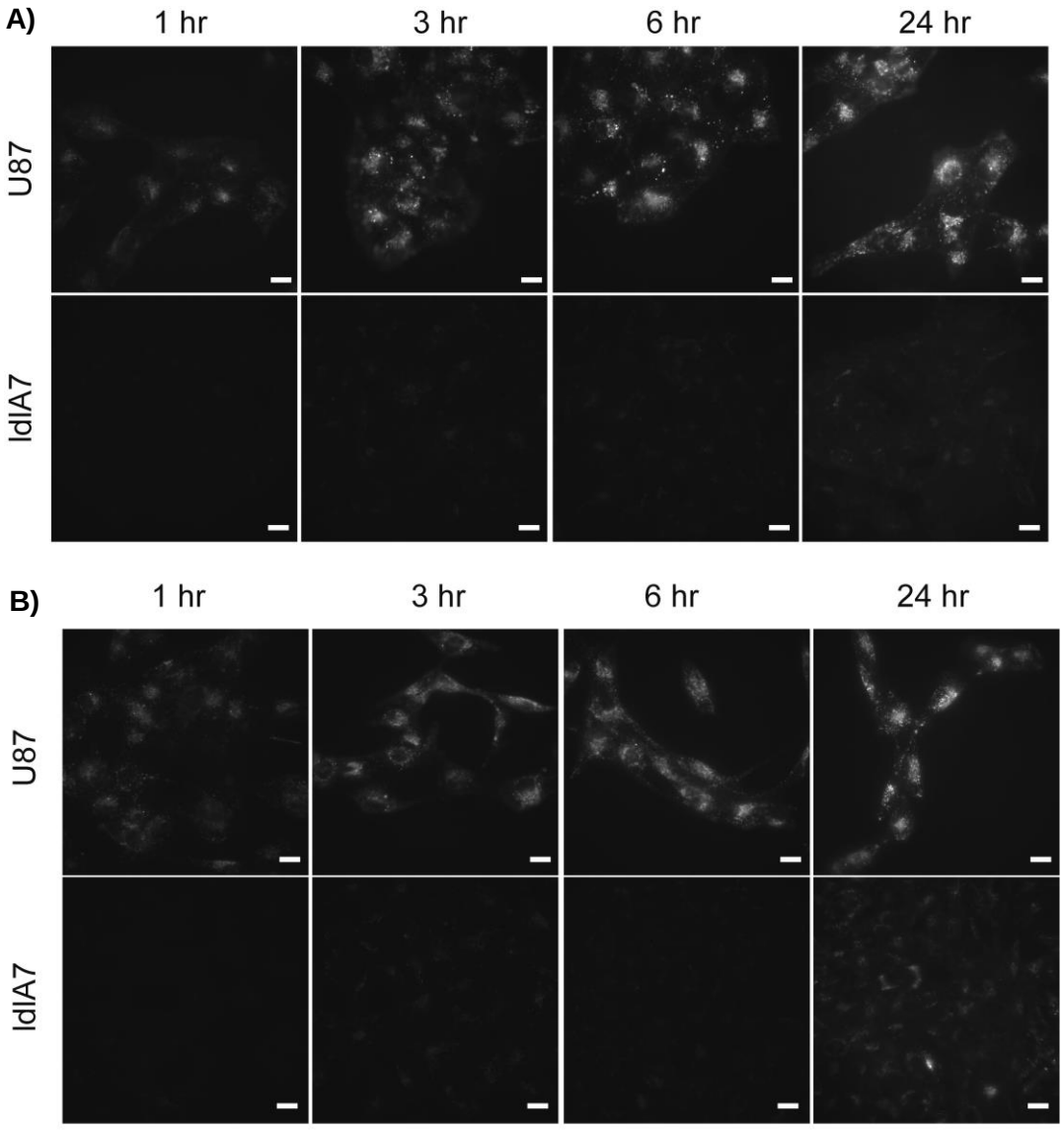

Figure S8: Time-dependent uptake of pyE-LN-D (a) and pyE-LN-CO in U87 (high LDLR expression) and ldlA7 (low LDLR expression) cells. The cells were treated with a porphyrin concentration of 5 uM for 1, 3, 6, or 24 hours prior to washing and imaging via fluorescence microscopy. The porphyrin signal shown above was visualized using a Cy5 filter (628/40 nm excitation, 692/40 nm emission). With equivalent light exposure, higher porphyrin fluorescence signal was observed in the LDLR-expressing U87 cells with increasing treatment times, while fluorescence signal emanating from treated ldlA7 cells was negligibly visible until 24 hours of treatment. Scale bars = 20 μm.

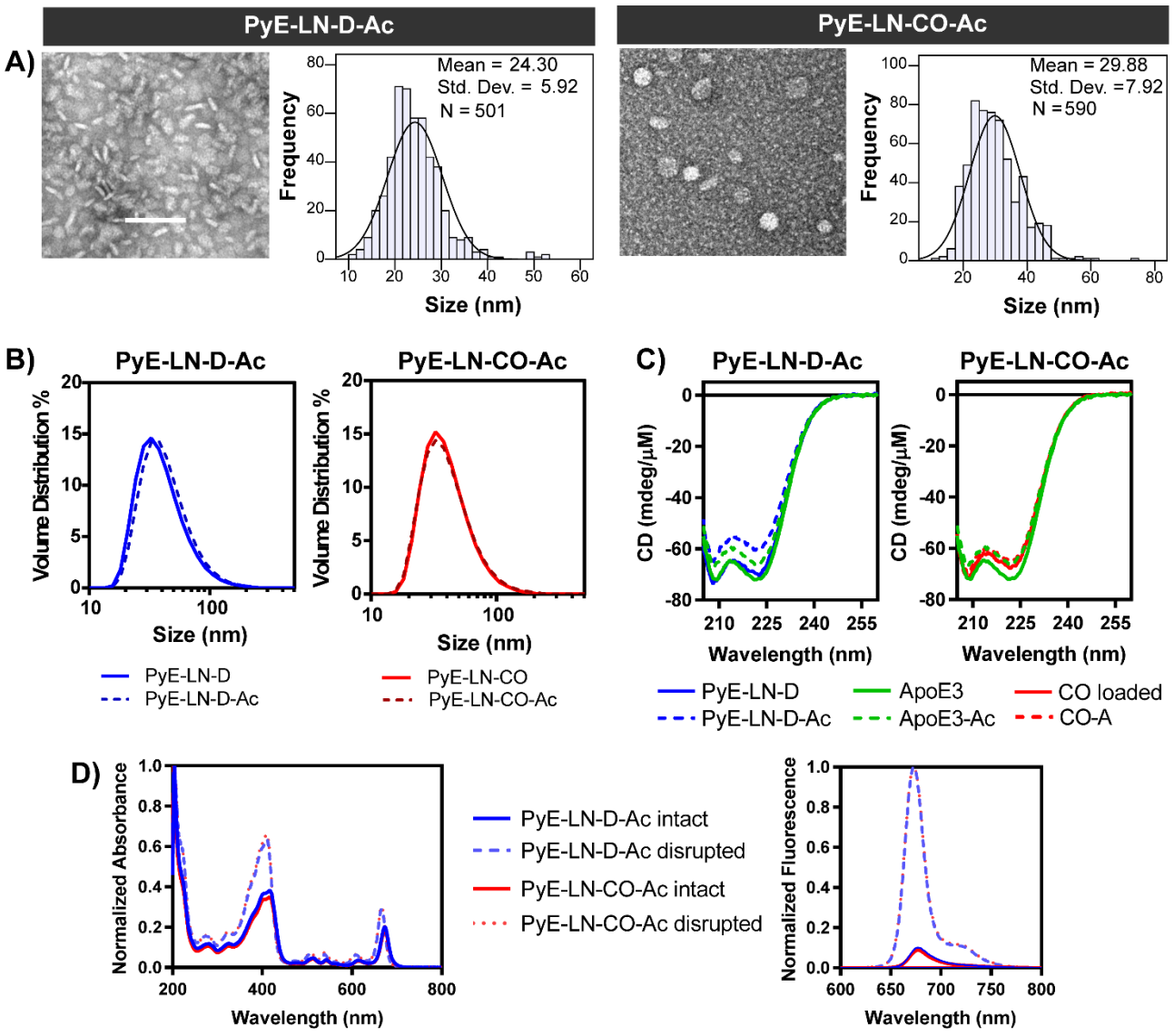

Characterization	PyE-LN-D-Ac	PyE-LN-CO-Ac
Size by TEM (nm)	24 ± 6 (28 ± 8)	30 ± 8 (29 ± 9)
Z-avg (nm)	22.33 (23.71)	61.79 (62.62)
PDI	0.186 (0.183)	0.346 (0.343)
Q_y intact	673 nm (673 nm)	673 nm (673 nm)
Q_y disrupted	666 nm (666 nm)	666 nm (666 nm)
Quenching efficiency (%)	88 (88)	90 (89)

Figure S9: In solution characterization of acetylated discoidal (pyE-LN-D-Ac) and CO-loaded (pyE-LN-CO-Ac) particles via TEM (a), DLS (b), CD (c), and spectrofluorotmetry and photometry (d). Acetylated particles had similar size, CD and optical properties as protein and porphyrin-lipid concentration-equivalent parent pyE-LN particles suspension as summarized in the illustrated table (values in parentheses are associated with the parent pyE-LN particles). Scale bar = 100 nm.

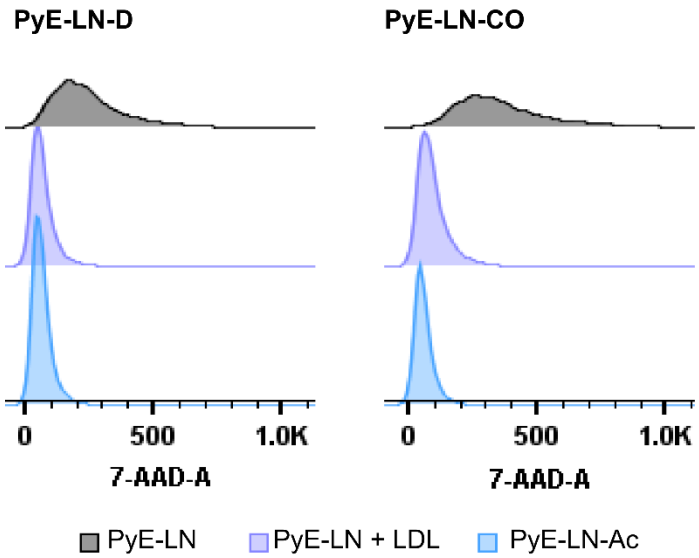

Figure S10: Representative flow cytometry histograms associated with in vitro pyE-LN uptake inhibition in U87 cells.

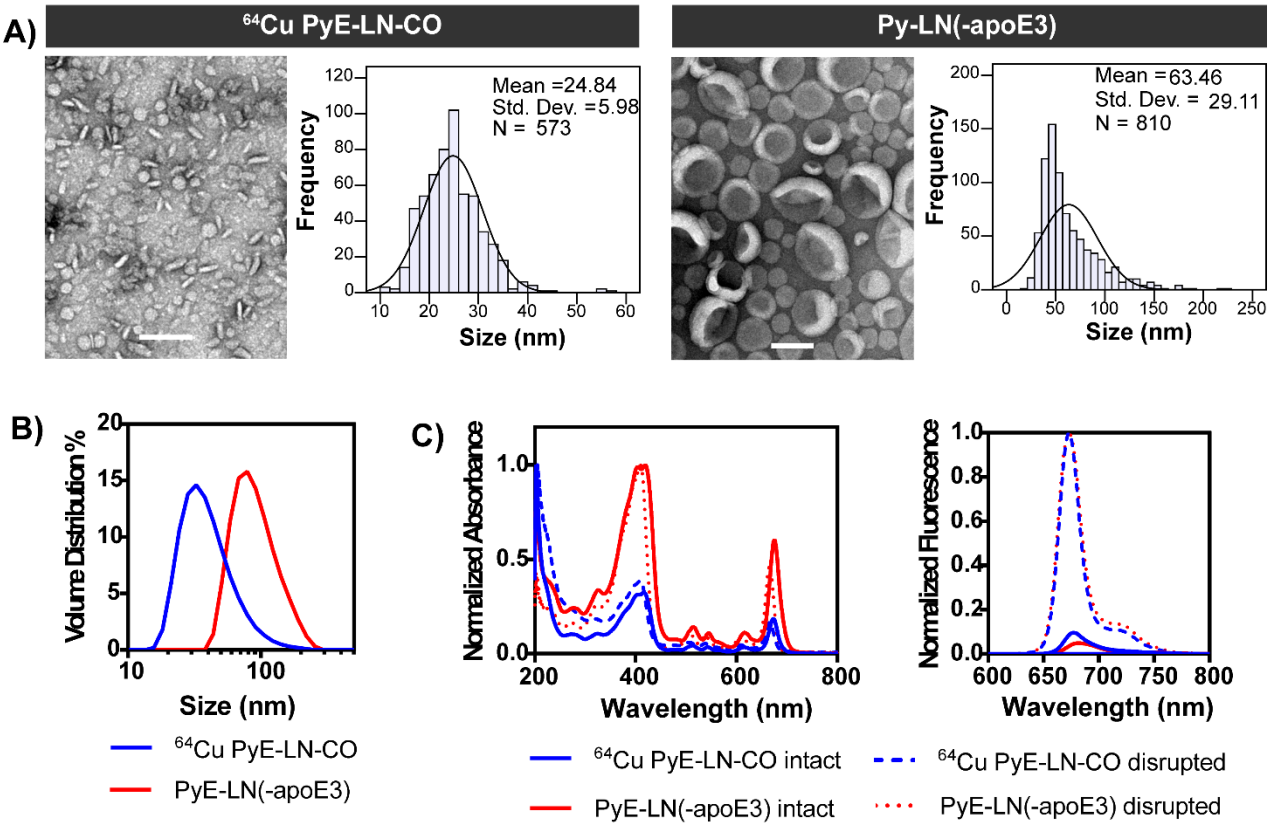

Characterization	^{64}Cu PyE-LN-CO	Py-LN(-apoE3)
Size by TEM (nm)	25 ± 6	69 ± 30
Z-avg (nm)	62.82	99.22
PDI	0.252	0.095
Q_y intact	674	674
Q_y disrupted	666	666
Quenching efficiency (%)	89	94
Radiolabeling efficiency (%)	100 ± 1.6	N/A

Figure S11: Characterization of pyE-LN particles utilized for in vivo studies. ^{64}Cu-PyE-LN-CO particles were allowed to undergo radioactive decay for two weeks prior to characterization alongside apoE3-devoid py-LN(-apoE3) particles via a) TEM, b) DLS, c) spectrofluorometry and spectrophotometry. Scale bar = 100 nm.